HAL
open science

Performance Analysis of Distributed Single Carrier Systems With Distributed Cyclic Delay Diversity

Kyeong Jin Kim, Marco Di Renzo, Hongwu Liu, Philip Orlik, H. Vincent Poor

To cite this version:

Kyeong Jin Kim, Marco Di Renzo, Hongwu Liu, Philip Orlik, H. Vincent Poor. Performance Analysis of Distributed Single Carrier Systems With Distributed Cyclic Delay Diversity. IEEE Transactions on Communications, 2017, 65 (12), pp.5514 - 5528. 10.1109/TCOMM.2017.2742511 . hal-01879964

HAL Id: hal-01879964

https://hal.science/hal-01879964v1

Submitted on 7 Jul 2020

HAL is a multi-disciplinary open access archive for the deposit and dissemination of scientific research documents, whether they are published or not. The documents may come from teaching and research institutions in France or abroad, or from public or private research centers.

L'archive ouverte pluridisciplinaire **HAL**, est destinée au dépôt et à la diffusion de documents scientifiques de niveau recherche, publiés ou non, émanant des établissements d'enseignement et de recherche français ou étrangers, des laboratoires publics ou privés.

Performance Analysis of Distributed Single Carrier Systems with Distributed Cyclic Delay Diversity

Kyeong Jin Kim, *Senior Member, IEEE,* Marco Di Renzo, *Senior Member, IEEE,*
Hongwu Liu, *Member, IEEE*, Philip V. Orlik *Senior Member, IEEE,* and
H. Vincent Poor *Fellow, IEEE*

***Abstract*—This paper investigates a distributed cyclic delay diversity (CDD) transmission scheme for cyclic-prefixed single carrier systems in non-identically and identically distributed frequency selective fading channels. The distinguishable feature of the proposed scheme lies in providing a transmit diversity gain while reducing the burden of estimating the channel state information (CSI), which is a challenging task in distributed and cooperative systems. To effectively use the distributed CDD scheme at the transmitters, two sufficient conditions are derived to eliminate the intersymbol interference at the receiver and leveraged to convert the multi-input single-output channel into a single-input single-output channel. These conditions allow the system to achieve the maximum diversity for frequency selective fading channels at a full rate. To achieve this maximum diversity, a fixed number of CDD transmitters is selected based on the channel conditions, symbol block size, and maximum time dispersion of the channel, and a new two-stage transmission mode is proposed. Based on the distributed CDD and the proposed selection schemes, a new expression for the signal-to-noise ratio at the receiver is obtained with the aid of order statistics, and then closed-form expressions for the outage probability and average symbol error rate (ASER) are derived. As far as the identically-distributed frequency selective fading channel model is concerned, the achievable maximum diversity gain is proved, with the aid of asymptotic analysis, to be equal to the product of the total number of transmitters in the system and the number of multipath components. Link-level simulations are also conducted to validate the mathematical expressions of outage probability, ASER, and maximum achievable diversity gain.**

***Index Terms*—Distributed single carrier system, cyclic delay diversity, diversity order, transmitter selection, frequency selective fading.**

I. Introduction

UNDER the assumption that exact channel state information (CSI) is available at the transmitter, the maximum ratio transmission (MRT) scheme [1], [2] has been proposed for exploiting the availability of multiple transmit antennas at each transmitter. In particular, by applying a transmit weight vector that maximizes the signal-to-noise ratio (SNR) [1], [2], better receiver performance can be achieved by virtue of a diversity gain proportional to the number of transmit antennas. Under the same conditions, MRT has been applied among distributed transmitters as well [3], in order to achieve a diversity order proportional to the number of cooperating transmitters. A distributed space-time-coded (STC) cooperative diversity scheme has been proposed in [4] and [5]. However, full rate orthogonal space-time block codes (STBCs) do not exist for a general number of distributed transmitters.

Since acquiring CSI is a challenging task in distributed cooperative systems, we consider, in the present paper, a more practical transmit diversity scheme, which is referred to as distributed cyclic delay diversity (CDD)[1] [6]–[10]. Owing to its compatibility with the Orthogonal Frequency Division Multiplexing (OFDM) transmission scheme and thanks to its reduced hardware complexity [8], CDD has been adopted in several wireless communication systems that are based on the 802.11ac [11], 802.11n [12], and Long-Term Evolution (LTE) protocols [13]. As for OFDM transmission, it is usually required to use forward error correction (FEC) codes in order to convert spatial diversity into frequency diversity.

Cyclic prefixed single-carrier (CP-SC) transmission [14] has been proposed as a good candidate scheme for several wireless systems [15]–[20], including cooperative relaying [15]–[18], spectrum sharing systems [19] and physical layer security [20]. In contrast to OFDM transmission, CP-SC transmission exhibits a reduced sensitivity to frequency offset errors, a lower peak-to-average power ratio (PAPR), and a reduced power-backing off. In addition, it alleviates the dynamic range requirements of the linear amplifiers [6], [14], [15].

Recently, several works [6], [7], [9], [10] have attempted to exploit CDD transmission for application to CP-SC systems. Notably, the block iterative generalized decision feedback equalizer (BI-GDFE) was proposed as an effective means for cancelling the interference [6]. Its maximum achievable diversity order, however, was not studied. In [7], on the other hand, the authors proved that the BI-GDFE system is capable of achieving the maximum diversity gain only if the transmission rate is no greater than a given threshold. Other works have, however, proved that CDD-based CP-SC systems can achieve the maximum diversity gain at full rate [9], [10]. In [9], in particular, the authors proposed a method forming

Manuscript received April 20, 2017; revised July 4, 2017; accepted August 8, 2017. The editor coordinating the review of this paper and approving it for publication was Prof. W. Chen.

K. J. Kim and P. V. Orlik are with Mitsubishi Electric Research Laboratories (MERL), Cambridge, MA, USA (e-mail: {kkim,porlik}@merl.com).

M. D. Renzo is with the Laboratoire des Signaux et Systèmes, CNRS, CentraleSupélec, Univ Paris Sud, Université Paris-Saclay, 3 rue Joliot Curie, Plateau du Moulon, 91192, Gif-sur-Yvette, France. (e-mail: marco.direnzo@l2s.centralesupelec.fr).

H. Liu is with the Department of Information and Communication Engineering, Inha University, South Korea. He is also with Shandong Jiaotong University, China. (e-mail: hong.w.liu@hotmail.com).

H. V. Poor is with the Department of Electrical Engineering, Princeton University, Princeton, NJ (e-mail: poor@princeton.edu).

[1]Since we apply CDD between cooperating transmitters, we call the proposed CDD as the distributed CDD.

an equivalent channel matrix for CDD with a proper choice of the delay. In [10], in addition, the CDD scheme was combined with relay selection for attaining the maximum diversity gain in Rayleigh fading channels.

Without the need of channel equalization [6], [21], research works in [15] and [22] have shown that the maximum diversity of cooperative CP-SC systems over frequency selective fading channels is jointly determined by multiuser diversity and multipath diversity. For two-hop cooperative relaying systems, best relaying selection and best terminal selection are respectively proposed in [15] and [22] for the independent and identically distributed (i.i.d.) fading channel. To achieve the maximum diversity, they both assume perfectly known CSI in the system. However, since either a single relay or terminal is selected for cooperation, its achievable coding gain is limited. Based on the above state of the art of research on CDD-based CP-SC systems, it can be concluded that the existing studies are applicable to the analysis of non-cooperative transmitters equipped with multiple transmit antennas. In the present paper, on the other hand, we focus our attention on systems with cooperative (or distributed) single-antenna, and hence low-complexity, transmitters. A major objective of our research work, more specifically, is to propose a CDD-based CP-SC system that is capable of achieving the maximum diversity without necessitating CSI either at the control unit (CU) or at the transmitters. In our system model, the CU employs the distributed CDD scheme among the transmitters. In light of this, the channels among the transmitters and the receiver of interest can be assumed to be independent but non-identically distributed (i.n.i.d.). In the present paper, as a consequence, an i.n.i.d. frequency selective fading channel model is assumed, which makes the performance evaluation of CDD-based CP-SC systems a challenging mathematical problem. To the best of the authors' knowledge, the mathematical analysis of this system model is not available in the open technical literature.

More specifically, the novel contributions of the present paper can be summarized as follows:

1) We propose a new cooperative CP-SC system that employs the distributed CDD scheme with a systematic delay assignment. In particular, we assume a general system model where only a subset of the available transmitters cooperatively apply the distributed CDD scheme. The selected transmitters are identified based on the maximum time dispersion of the channel and size of the block symbol for CP-SC transmission. A two-stage selection process is proposed in order to select the collaborative transmitters.
2) Inspired by the work in [9] and [10], we derive two sufficient conditions for achieving the maximum diversity order at full rate that is offered by CP-SC transmission.
3) In the general i.n.i.d. frequency selective fading channel, we derive closed-form expressions of the outage probability and average symbol error rate (ASER) when either one or two CDD transmitters are available. As far as the analysis of system models with a larger number of CDD transmitters is concerned, we provide closed-form expressions of the same performance metrics in the i.i.d. frequency selective fading channel. This is due to the mathematical intractability of i.n.i.d. frequency selective fading channels if more than two CDD transmitters are considered. Based on the proposed mathematical frameworks, we prove that the maximum achievable diversity order is equal to the product of the number of available transmitters and multipath components.

The rest of the present paper is organized as follows. In Section II, the system and channel models are summarized. The distributed CDD-based CP-SC system model is introduced as well. In Section III and Section IV, the outage probability and ASER are computed in i.n.i.d. and i.i.d. frequency selective fading channels, respectively. Simulation results are presented in Section V and conclusions are drawn in Section VI.

Notation: The superscript $(\cdot)^H$ denotes complex conjugate transposition; $< . >_Q$ denotes the modulo operation with base Q; $\boldsymbol{I}_N$ denotes an $N \times N$ identity matrix; $\mathbf{0}$ denotes an all-zero matrix of appropriate dimensions; $\mathcal{CN}\left(\mu, \sigma^2\right)$ denotes the complex Gaussian distribution with mean μ and variance σ^2; $\mathbb{C}^{m\times n}$ denotes the vector space of all $m \times n$ complex matrices; $F_\varphi(\cdot)$ denotes the cumulative distribution function (CDF) of the random variable (RV) φ, whose probability density function (PDF) is denoted by $f_\varphi(\cdot)$; $\binom{n}{k} \triangleq \frac{n!}{(n-k)!k!}$ denotes the binomial coefficient; $\boldsymbol{a}(l)$ denotes the lth element of vector $\boldsymbol{a}$ and $\boldsymbol{A}(k,l)$ denotes the (k,l) element of matrix $\boldsymbol{A}$.

II. System and Channel Model

A block diagram of the considered cooperative system is provided in Fig. 1. The CU provides perfect backhaul connections $\{b_m\}_{m=1}^M$ to M single-antenna transmitters $\{\mathrm{TX}\}_{m=1}^M$. This assumption originates from the fact that remote radio head (RRH) types of transmitters are assumed[2]. Likewise, the receiver, R, is equipped with a single receive antenna. We assume two types of channel models: (1) i.n.i.d. frequency selective fading channels, which, in general, are comprised of a different number of multipath components. Since the single antenna equipped transmitters can be distributed at random in the region of interest, different path losses and different fading severity are assumed. A distance-dependent path loss component is also used to model large scale fading; (2) i.i.d. frequency selective fading channels, which are made of the same number of multipath components. In this case, the transmitters are located at the same distance from the receiver. This channel model, despite being simplified, is often considered for getting some insight for system design and optimization and it is widely used in the literature.

Since there are $M \geq K$ transmitters in the system, the CU needs to select those that will take part to the CDD processing. To this end, we propose the transmitter selection process discussed in the next sections.

A. Pilot Transmission for Initialization

Due to the presence of a larger number of distributed transmitters compared with the number of transmitters that

[2]As for the use of a baseband unit (BBU) instead of the CU, perfect fronthaul links are assumed from the BBU to RRHs.

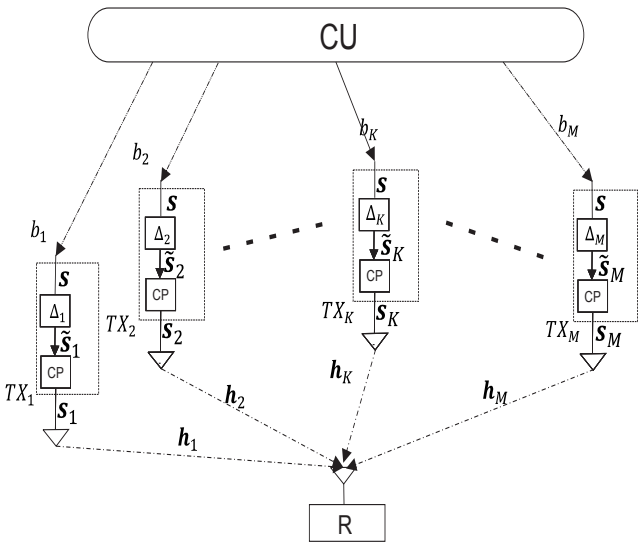

Fig. 1. Block diagram of the proposed distributed CDD-based cooperative CP-SC system. All the single antenna equipped transmitters are connected to the CU via perfect backhaul links $\{b_m\}_{m=1}^{M}$ and communicate with the receiver R through independent frequency selective fading channels $\{\boldsymbol{h}_m\}_{m=1}^{M}$. Out of $M \geq K$ transmitters, only K transmitters take part in the data transmission with the aid of CDD-aided processing. So, $M-K$ non-CDD transmitters do not participate to data transmission.

employ CDD processing, two questions need to be answered:

Q_1 : How to choose only K CDD transmitters out of M $(M \geq K)$ available transmitters?

Q_2 : How to assign a CDD delay Δ_k to the CDD transmitter TX_k?

To answer these questions, we assume that pilot symbols can be used at the transmitter and that they are known at the receiver. The signal received at the receiver and transmitted from the kth transmitter can be written as follows:

$$\boldsymbol{p}_k = \sqrt{P_T \alpha_k} \boldsymbol{H}_k \boldsymbol{p} + \boldsymbol{z}_R \tag{1}$$

where P_T is the transmission power of each transmitter, α_k is the path loss component of the independent channel $\boldsymbol{h}_k$, $\boldsymbol{H}_k \in \mathbb{C}^{Q\times Q}$ is a right circulant matrix whose (j,l)th element is $\boldsymbol{H}_k(j,l) = \boldsymbol{h}_k(< j-l >_Q)$, and $\boldsymbol{z}_R$ is the receiver noise $\boldsymbol{z}_R \sim \mathcal{CN}(\boldsymbol{0}, \sigma_z^2 \boldsymbol{I}_Q)$. A common pilot symbol block is denoted by $\boldsymbol{p} \in \mathbb{C}^{Q\times 1}$ with $E\{\boldsymbol{p}\} = \boldsymbol{0}$, $E\{\boldsymbol{p}\boldsymbol{p}^H\} = \boldsymbol{I}_Q$. The block size of $\boldsymbol{p}$ is denoted by Q. Since known pilot symbols are used, no detection is necessary at the receiver. In addition, by employing appropriate channel sounding schemes, the receiver is assumed to have exact knowledge of the number of multipath components of each channel $\boldsymbol{h}_k$.

From (1), the SNR at the receiver is as follows [15]:

$$\gamma_k \triangleq \frac{P_T \alpha_k \|\boldsymbol{h}_k\|^2}{\sigma_z^2} = \tilde{\alpha}_k \|\boldsymbol{h}_k\|^2 \tag{2}$$

where $\tilde{\alpha}_k \triangleq \frac{P_T \alpha_k}{\sigma_z^2}$.

The M available SNRs are arranged in ascending order of magnitude as follows [23], [24]:

$$0 \leq \gamma_{(1)} \leq \gamma_{(2)} \leq \cdots \leq \gamma_{(M)} \tag{3}$$

and their corresponding indices are denoted by $\mathbb{X}_I \triangleq [(1),(2),\cdots,(M)]$. To reduce the feedback overhead from the receiver to the CU, the receiver feeds back $\mathbb{X}_I$ and the maximum number of multipath components estimated from channel sounding, namely, $N_h = \max(N_1,\ldots,N_K)$, to the CU.

The CU is assumed to be aware of N_h and of the CP length, N_p. Thus, the CDD delay length, Δ_i, can be determined from the following two conditions:

$$C_1 : N_p = N_h, \tag{4}$$

$$C_2 : \Delta_i = (i-1)N_p \tag{5}$$

where C_1 is needed to remove the intersymbol interference (ISI) caused by the CP-SC transmission [15], and C_2 is required to form a non-overlapping equivalent channel vector that allows us to convert the multi-input single-output (MISO) channel into a single-input single-output (SISO) channel [9]. More precisely, the ISI can be removed if $N_p \geq N_h$. Since it is preferable to keep the CP length as small as possible compared to the symbol block size Q, we consider $N_p = N_h$.

Based on C_1 and C_2, we propose to determine the number of CDD transmitters, K, as a function of the symbol block size, Q, and the maximum number of multipath components, as follows:

$$K = 1 + \left\lfloor \frac{Q}{N_p} \right\rfloor \tag{6}$$

where $\lfloor\cdot\rfloor$ denotes the floor function.

Since we assume $M \geq K$, the CU needs to select the K CDD transmitters that are specified by the last K elements of $\mathbb{X}_I$ and form a table of CDD delays, $\mathbb{X}_\Delta \triangleq \{\Delta_1,\ldots,\Delta_{K-1},\Delta_K\}$, which is used for assigning the CDD delays to the CDD transmitters. The main objective is, in fact, uniquely assigning one out of the K delays in $\mathbb{X}_\Delta$ to a given CDD transmitter. To this end, consider the K chosen CDD transmitters. Assume that Q transmission symbols, $\{s_1,\ldots,s_Q\}$, are transmitted sequentially from the CU or BBU to all the transmitters. Each CDD transmitter collects them to form a transmission symbol block $\boldsymbol{s} = [s_1,...,s_Q]^T \in \mathbb{C}^{Q\times 1}$, where we assume that $E\{\boldsymbol{s}\} = \boldsymbol{0}$ and $E\{\boldsymbol{s}\boldsymbol{s}^H\} = \boldsymbol{I}_Q$. Let Δ_k be the unique CDD delay assigned to the kth CDD transmitter. The exact value of Δ_k is discussed in Corollary 1 below. The kth CDD transmitter applies circular shifting operations by using its assigned CDD delay Δ_k, which can be expressed by applying the permutation shifting matrix $\boldsymbol{P}_Q^{\Delta_k}$. In particular, the matrix $\boldsymbol{P}_Q^{\Delta_k}$ is obtained by circularly shifting down the identity matrix $\boldsymbol{I}_Q$ by Δ_k. For instance, $\boldsymbol{P}_{Q=4}^{\Delta_k=1}$ is given by

$$\boldsymbol{P}_{Q=4}^{\Delta_k=1} = \begin{bmatrix} 0 & 1 & 0 & 0 \\ 0 & 0 & 1 & 0 \\ 0 & 0 & 0 & 1 \\ 1 & 0 & 0 & 0 \end{bmatrix}. \tag{7}$$

Let us apply the QR decomposition (QRD) to the right circulant matrices $\boldsymbol{H}_{cir}$ and $\boldsymbol{H}_{cir}^{\Delta_k} \triangleq \boldsymbol{H}_{cir}\boldsymbol{P}_Q^{\Delta_k}$. We obtain $\boldsymbol{H}_{cir}^{\Delta_k} = \boldsymbol{Q}^{\Delta_k}\boldsymbol{R}^{\Delta_k}$, where

$$\boldsymbol{Q}^{\Delta_k} = \boldsymbol{P}_Q^{\Delta_k}\boldsymbol{Q}, \text{ and } \boldsymbol{R}^{\Delta_k} = \boldsymbol{R} \tag{8}$$

which shows that the upper triangular matrix, $\boldsymbol{R}^{\Delta_k}$, obtained from the QRD of the column permutated circulant matrix is independent of the column permutation, whereas the unitary matrix, $\boldsymbol{Q}^{\Delta_k}$, is obtained by pre-multiplying the permutation matrix by $\boldsymbol{Q}$[3]. With these prerequisites, the following corollary holds.

Corollary 1: Let the delays of the K CDD transmitters satisfy the conditions C_1 and C_2. Then, provided that each transmitter is assigned a different delay, different assignments of the cyclic delays to the CDD transmitters result in the same performance if a maximum likelihood detector (MLD) [15] is used at the receiver.

Proof: See Appendix A. ■

Corollary 1 implies that the system performance, which depends on trace $\left((\boldsymbol{H}_{cir}^{\Delta_k})^H \boldsymbol{H}_{cir}^{\Delta_k}\right)$, is independent of the selection priority of the delays. For example, the CU has the freedom of assigning the delay Δ_k to the CDD transmitter TX_k without any performance loss. In the sequel, this assumption is retained for simplicity but without loss of generality. Based on Corollary 1, as a result, the CU needs only N_h and $\mathbb{X}_I$ for applying the proposed CDD-based CP-SC transmission scheme.

B. Information Data Transmission via Distributed CDD

Let us apply the permutation shifting matrix to the kth CDD transmitter. The corresponding symbol $\tilde{\boldsymbol{s}}$ can be formulated as: $\tilde{\boldsymbol{s}}_k = \boldsymbol{P}_Q^{\Delta_k}\boldsymbol{s}$, where $\boldsymbol{s} \in \mathbb{C}^{Q\times 1}$. Before transmission, a CP that contains the last N_p symbols of $\tilde{\boldsymbol{s}}_k$, is added to the front of $\tilde{\boldsymbol{s}}_k$. The obtained symbol, $\boldsymbol{s}_k$, is sent through a frequency-selective fading channel that is denoted by $\boldsymbol{h}_k$ and is assumed to have N_k multipath components.

At the receiver, after removing the CP, the signal can be formulated as

$$\boldsymbol{r} = \sum_{k=1}^{K} \sqrt{P_T\alpha_k}\boldsymbol{H}_k\boldsymbol{P}_Q^{\Delta_k}\boldsymbol{s} + \boldsymbol{z}_R \tag{9}$$

where the additive noise is $\boldsymbol{z}_R \sim \mathcal{CN}(\boldsymbol{0}, \sigma_z^2\boldsymbol{I}_Q)$. Since the product of two right circulant matrices, $\boldsymbol{H}_k$ and $\boldsymbol{P}_Q^{\Delta_k}$, is another right circulant matrix, with the aid of (5), (9) can be expressed as follows:

$$\boldsymbol{r} = \boldsymbol{H}^{\text{CDD}}\boldsymbol{s} + \boldsymbol{z}_R \tag{10}$$

where $\boldsymbol{H}^{\text{CDD}}$ is an equivalent channel matrix comprising the frequency fading channels from the K CDD transmitters to the receiver. Its first column vector is as follows:

$$\begin{aligned}\boldsymbol{h}^{\text{CDD}} \triangleq \big[&\sqrt{P_T\alpha_1}(\boldsymbol{h}_1)^T, \boldsymbol{0}_{1\times(N_p-N_1)}, \ldots,\\ &\sqrt{P_T\alpha_K}(\boldsymbol{h}_K)^T, \boldsymbol{0}_{1\times(N_p-N_K)}\big]^T \in \mathbb{C}^{Q\times 1}.\end{aligned} \tag{11}$$

Since right circulant matrices are determined by their first column vector, then $\boldsymbol{h}^{\text{CDD}}$ completely specifies the equivalent channel matrix $\boldsymbol{H}^{\text{CDD}}$.

From the equivalent expression of the received signal $\boldsymbol{r}$, we can observe the following facts:

1) The received signal does not include interference from other CDD transmitters. This is obtained by virtue of the properly designed CDD delays Δ_k. As a result, the MISO channel is converted into a SISO channel for distributed CP-SC transmission. Since each channel vector comprises N_p elements, additional zeros are required in forming $\boldsymbol{h}^{\text{CDD}}$.
2) Maximum transmit diversity can be achieved by employing the proposed distributed CDD scheme which specifies the CDD delay according to two sufficient conditions specified by Eqs. (4) and (5). This is proved mathematically in the following sections.

III. Performance Analysis in I.N.I.D. Frequency Selective Fading Channels

To investigate the performance of the proposed distributed CCD-based CP-SC transmission scheme, the distribution of the SNR at the receiver needs to be computed.

A. SNR at the Receiver

From (9), the SNR [15] over the channel from the kth CDD transmitter to the receiver can be formulated as follows:

$$\gamma_k = \frac{P_T\alpha_k\|\boldsymbol{h}\|^2}{\sigma_z^2} = \tilde{\alpha}_k\|\boldsymbol{h}_k\|^2 \tag{12}$$

which coincides with (2). The CDF and PDF of γ_k are, respectively, given by

$$\begin{aligned}F_k(x) &= 1 - e^{-\frac{x}{\tilde{\alpha}_k}}\sum_{l=0}^{N_k-1}\frac{1}{l!}\Big(\frac{x}{\tilde{\alpha}_k}\Big)^l \text{ and}\\ f_k(x) &= \frac{x^{N_k-1}}{\Gamma(N_k)(\tilde{\alpha}_k)^{N_k}}e^{-\frac{x}{\tilde{\alpha}_k}}\end{aligned} \tag{13}$$

where $\Gamma(\cdot)$ denotes the gamma function. Based on (9), the aggregated SNR from the K CDD transmitters is given by

$$\begin{aligned}S^K &= \sum_{k=1}^{K}\tilde{\alpha}_{(M-K+k)}\sum_{l=1}^{N_{(M-K+k)}}|\boldsymbol{h}_{(M-K+k)}(l)|^2\\ &= \sum_{k=1}^{K}\gamma_{(M-K+k)}.\end{aligned} \tag{14}$$

It is important to mention that the selected K CDD transmitters provide the largest K SNRs to the receiver. This implies that the analysis of (14) requires the mathematical tool of order statistics. In other words, $\gamma_{(M)}$ is the largest SNR, $\gamma_{(M-1)}$ is the second largest SNR, etc. Thus, $\sum_{k=1}^{K}\gamma_{(M-K+k)}$ is the sum of the K largest SNRs. This implies that the SNRs in (14) are correlated and, thus, the mathematical analysis of (14) is a non-trivial problem.

Let us arrange the SNRs in increasing order of magnitude, i.e., $\gamma_{(M-K+1)} < \gamma_{(M-K+2)} < \ldots < \gamma_{(M)}$. The joint PDF of $\gamma_{r_1}\triangleq\gamma_{(M-K+1)}, \gamma_{r_2}\triangleq\gamma_{(M-K+2)}, \ldots, \gamma_{r_K}\triangleq\gamma_{(M)}$ can be written as [24]:

$$f_{r_1,r_2,\ldots,r_K}(x_1, x_2, \ldots, x_K) = \frac{1}{(M-K)!}\text{Per}\boldsymbol{A}_K \tag{15}$$

[3]If the diagonal components of the matrix $\boldsymbol{R}^{\Delta_k}$ are all positive, these two prerequisites are true.

where

$$\boldsymbol{A}_K \triangleq \begin{bmatrix} F_1(x_1) & f_1(x_1) & \dots & f_1(x_K) \\ F_2(x_1) & f_2(x_1) & \dots & f_2(x_K) \\ \vdots & \vdots & \vdots & \vdots \\ F_M(x_1) & f_M(x_1) & \dots & f_M(x_K) \\ \underbrace{M-K} & \underbrace{1} & \underbrace{1} & \underbrace{1} \end{bmatrix} \tag{16}$$

and $F_k(\cdot)$ and $f_k(\cdot)$ are the CDF and PDF of γ_k, i.e., the kth SNR without CDD operation. Their expressions are provided in (13). Also, let us define the matrix $\begin{bmatrix} a_{11} & a_{12} \\ \vdots & \vdots \\ a_{M1} & a_{M2} \\ \underbrace{i} & \underbrace{j} \end{bmatrix}$ containing i copies of the first column vector $[a_{11}, \dots, a_{M1}]^T$ and j copies of the second column vector $[a_{12}, \dots, a_{M2}]^T$. The permanent of a square matrix $\boldsymbol{A}$, denoted by $\mathrm{Per}\boldsymbol{A}$, is defined similar to the matrix determinant except for the fact that all signs are positive [23], [24]. If a square matrix $\boldsymbol{A}$ is considered, for example, $\boldsymbol{A} = \begin{bmatrix} a & b \\ c & d \\ \underbrace{1} & \underbrace{1} \end{bmatrix}$, we have $\mathrm{Per}\boldsymbol{A} = ad + bc$.

With the aid of some alegraic manipulations, a desired compact expression for $\mathrm{Per}\tilde{\boldsymbol{A}}_K \triangleq \frac{\mathrm{Per}\boldsymbol{A}_K}{(M-K)!}$ can be shown to be (17) at the next page. For ease of analysis, we introduce the notation $\mathbb{X}_M \triangleq \{1, \dots, M\}$ and $\mathbb{X}_p \triangleq \mathbb{X}_M - \{i_1, \dots, i_{M-K}\}$. Also, the list of all possible permutations of the elements of $\mathbb{X}_p$ is denoted by $\mathbb{P}_p \triangleq \mathrm{Perms}(\mathbb{X}_p)$, where q denotes the qth permutation of $\mathbb{P}_p$. In addition, $k_{l,q}$ denotes the lth element of permutation q. By applying the binomial and multinomial theorems [25, eq. (1.111)], (17) can be written as (18) at the next page. In (18), we have defined $D_1 \triangleq \frac{q_1}{\tilde{\alpha}_{i_1}} + \dots + \frac{q_{M-K}}{\tilde{\alpha}_{i_{M-K}}} + \frac{1}{\tilde{\alpha}_{k_{1,q}}}$, $\tilde{m}_1 \triangleq \tilde{q}_1 + \dots + \tilde{q}_{M-K} + N_{k_{1,q}}$, and $\tilde{q}_l \triangleq \sum_{t_l=0}^{N_{i_l}-1} t_l q_{l,t_l+1}$. Also, $\sum_{\substack{q_{j,1},\dots,q_{j,N_{i_j}} \\ q_{j,1}+\dots+q_{j,N_{i_j}}=q_j}}$ denotes the sum for all set of positive indices $\{q_{j,1}, \dots q_{j,N_{i_j}}\}$ satisfying $q_{j,1} + \dots + q_{j,N_{i_j}} = q_j$ with the possible range of $0 \le q_{j,m} \le q_j,\ \exists j, \forall m$.

From (18), the moment generating function (MGF) of the RV S^K can be computed as follows:

$$\Phi_{S^K}(s) = \int_0^{x_2} \int_0^{x_3} \dots \int_0^{x_K} \int_0^{\infty} e^{-s(x_1+\dots+x_K)} \mathrm{Per}\tilde{\boldsymbol{A}}_K dx_1 dx_2 \dots dx_{K-1} dx_K. \tag{19}$$

The MGF in (19) necessitates the computation of $(K-1)$-fold nested integrals, whose solution does not exist for general values of K in the considered i.n.i.d. frequency selective fading channel model. In the rest of this section, therefore, we focus our attention only on the case studies $K \in \{1, 2\}$, for which closed-form solutions can be found. In Section IV, on the other hand, we consider the i.i.d. frequency selective fading channel model for which closed-form expressions of the MGF can be found for general values of K.

Theorem 1: The CDF of the aggregated received SNR from two CDD transmitters in i.n.i.d. frequency selective fading channels with $N_h = N_k, \forall k$ is given by (20) at the next page. In (20), we have defined $D_2 \triangleq \frac{1}{\tilde{\alpha}_{k_{2,q}}}$ and $\gamma_l(\cdot,\cdot)$ denotes the lower-incomplete gamma function.

Proof: See Appendix B. ■

If $K = 1$, i.e., a single CDD transmitter is considered, $\mathrm{Per}\tilde{\boldsymbol{A}}_K$ is given by (21) at the next page. Note that (21) is the PDF of $\gamma_{(M)}$ and $S^{K=1}$. Different but equivalent expressions for $\gamma_{(M)}$ are derived in [26]. From (21), the CDF of $S^{K=1}$ can be formulated as the expression in (22) provided at the next two pages.

B. Outage Probability

From the CDF, the outage probability can be readily formulated in closed-form. For a given outage threshold, γ_{th}, the outage probability is as follows:

$$O_{\mathrm{out}}(\gamma_{\mathrm{th}}) = \begin{cases} F_{S^{K=1}}(\gamma_{\mathrm{th}}), & \text{for } K = 1, \\ F_{S^{K=2}}(\gamma_{\mathrm{th}}), & \text{for } K = 2. \end{cases} \tag{23}$$

It is worth noting that $F_{S^{K=1}}(\gamma_{\mathrm{th}})$ is the outage probability corresponding to the worst-case scenario for the proposed CDD-based CP-SC transmission scheme.

C. Average Bit Error Rate

According to [27], the ASER can be expressed, as a function of the CDF of the received SNR, as follows:

$$P_e = \frac{m_a\sqrt{m_b}}{2\sqrt{\pi}} \int_0^{\infty} x^{-1/2} F_{S^K}(x) e^{-x m_b} dx \tag{24}$$

where m_a and m_b are specified by the modulation scheme being used.

With the aid of the closed-form expressions of $F_{S^{K=1}}(x)$ and $F_{S^{K=2}}(x)$, an explicit expression of the ASER is provided in the following theorem.

Theorem 2: The closed-form expression of the worst ASER of the CDD-based CP-SC transmission scheme is given by (25) at the next two pages.

Proof: The computation of $P_e^{K=1}$ follows from the following notable integral:

$$\begin{aligned} & \frac{m_a\sqrt{m_b}}{2\sqrt{\pi}} \int_0^{\infty} x^{-1/2} \gamma_l(\tilde{m}_1, D_1 x) e^{-m_b x} dx \\ \overset{(a)}{=} & \frac{m_a\sqrt{m_b}}{2\sqrt{\pi}} \int_0^{\infty} x^{-1/2} e^{-m_b x} G_{1,2}^{1,1}\Big(D_1 x \Big| \begin{matrix} 1 \\ \tilde{m}_1, 0 \end{matrix}\Big) dx \\ \overset{(b)}{=} & \frac{m_a}{2\sqrt{\pi}} G_{2,2}^{1,2}\Big(\frac{D_1}{m_b} \Big| \begin{matrix} 1/2, 1 \\ \tilde{m}_1, 0 \end{matrix}\Big) \end{aligned} \tag{26}$$

where $G_{p,q}^{m,n}\Big(t \Big| \begin{matrix} a_1, ..., a_n, a_{n+1}, ..., a_p \\ b_1, ..., b_m, b_{m+1}, ..., b_q \end{matrix}\Big)$ denotes the Meijer G-function [25, eq. (9.301)]. In the derivation of (26), we use [28, eq.(06.06.26.0004.01)] in (a) and [29, eq. (2.24.3.1)] in (b). Replacing K_1 in (22) with (26), the final result in (25) follows. ■

$$\begin{aligned}\mathrm{Per}\tilde{\boldsymbol{A}}_K &= \sum_{\substack{i_1,i_2,\ldots,i_{M-K}\\ 1\le i_1<i_2<\ldots<i_{M-K}\le M}} \sum_{q\in\mathbb{P}_p} \prod_{j=1}^{M-K} F_{i_j}(x_1) f_{k_{1,q}}(x_1) \prod_{l=2}^{K} f_{k_{l,q}}(x_l) \\ &= \sum_{\substack{i_1,i_2,\ldots,i_{M-K}\\ 1\le i_1<i_2<\ldots<i_{M-K}\le M}} \sum_{q\in\mathbb{P}_p} \prod_{j=1}^{M-K} \Big(1 - e^{-\frac{x_1}{\tilde{\alpha}_{i_j}}} \sum_{l=0}^{N_{i_j}-1} \frac{(x_1)^l \tilde{\alpha}_{i_j}^{-l}}{\Gamma(l+1)}\Big) \frac{(x_1)^{N_{k_{1,q}}-1} e^{-\frac{x_1}{\tilde{\alpha}_{k_{1,q}}}}}{\Gamma(N_{k_{1,q}})(\tilde{\alpha}_{k_{1,q}})^{N_{k_{1,q}}}} \prod_{l=2}^{K} \frac{(x_l)^{N_{k_{l,q}}-1} e^{-\frac{x_l}{\alpha_{k_{l,q}}}}}{\Gamma(N_{k_{l,q}})(\tilde{\alpha}_{k_{l,q}})^{N_{k_{l,q}}}}. \end{aligned} \tag{17}$$

$$\begin{aligned}\mathrm{Per}\tilde{\boldsymbol{A}}_K = &\sum_{\substack{i_1,i_2,\ldots,i_{M-K}\\ 1\le i_1<i_2<\ldots<i_{M-K}\le M}} \sum_{q\in\mathbb{P}_p} \sum_{q_1=0}^{1} \cdots \sum_{q_{M-K}=0}^{1} \binom{1}{q_1} \cdots \binom{1}{q_{M-K}} (-1)^{q_1+\ldots+q_{M-K}} \\ &\sum_{\substack{q_{1,1},\ldots,q_{1,N_{i_1}}\\ q_{1,1}+\ldots+q_{1,N_{i_1}}=q_1}} \cdots \sum_{\substack{q_{M-K,1},\ldots,q_{M-K,N_{i_{M-K}}}\\ q_{M-K,1}+\ldots+q_{M-K,N_{i_{M-K}}}=q_{M-K}}} \prod_{j=1}^{M-K} \left(\frac{q_j!}{q_{j,1}!\ldots q_{j,N_{i_j}}!}\right) \\ &\prod_{j=1}^{M-K} \prod_{t_j=0}^{N_{i_j}-1} \Big(\frac{1}{t_j!}\Big)^{q_{j,t_j+1}} \prod_{j=1}^{M-K} \Big(\frac{1}{\tilde{\alpha}_{i,j}}\Big)^{\tilde{q}_j} \Big(\frac{1}{\tilde{\alpha}_{k_{1,q}}}\Big)^{N_{k_{1,q}}} \frac{e^{-x_1 D_1} x_1^{\tilde{m}_1-1}}{\Gamma(N_{k_{1,q}})} \prod_{l=2}^{K} \frac{(x_l)^{N_{k_{l,q}}-1} e^{-\frac{x_l}{\alpha_{k_{l,q}}}}}{\Gamma(N_{k_{l,q}})(\tilde{\alpha}_{k_{l,q}})^{N_{k_{l,q}}}}. \end{aligned} \tag{18}$$

$$\begin{aligned}F_{S^{K=2}}(x) = &\sum_{\substack{i_1,i_2,\ldots,i_{M-2}\\ 1\le i_1<i_2<\ldots<i_{M-2}\le M}} \sum_{q\in\mathbb{P}_p} \sum_{q_1=0}^{1} \cdots \sum_{q_{M-2}=0}^{1} \binom{1}{q_1} \cdots \binom{1}{q_{M-2}} (-1)^{q_1+\ldots+q_{M-2}} \\ &\sum_{\substack{q_{1,1},\ldots,q_{1,N_h}\\ q_{1,1}+\ldots+q_{1,N_h}=q_1}} \cdots \sum_{\substack{q_{M-2,1},\ldots,q_{M-2,N_h}\\ q_{M-2,1}+\ldots+q_{M-2,N_h}=q_{M-2}}} \prod_{j=1}^{M-K} \left(\frac{q_j!}{q_{j,1}!\ldots q_{j,N_h}!}\right) \\ &\prod_{j=1}^{M-2} \prod_{t_j=0}^{N_h-1} \Big(\frac{1}{t_j!}\Big)^{q_{j,t_j+1}} \prod_{j=1}^{M-2} \Big(\frac{1}{\tilde{\alpha}_{i,j}}\Big)^{\tilde{q}_j} \Big(\frac{1}{\tilde{\alpha}_{k_{1,q}}}\Big)^{N_h} \frac{\Gamma(\tilde{m}_1)}{\Gamma(N_h)} \Big(\frac{1}{\tilde{\alpha}_{k_{2,q}}}\Big)^{N_h} \\ &\Big[\sum_{f=1}^{\tilde{m}_1} (-1)^{\tilde{m}_1-f} (D_2-D_1)^{-(\tilde{m}_1+N_h-f)} \binom{\tilde{m}_1+N_h-f-1}{\tilde{m}_1-f} \frac{\gamma_l(f,D_1x)}{\Gamma(f)(D_1)^f} + \\ &\sum_{f=1}^{N_h} (-1)^{N_h-f} (D_1-D_2)^{-(\tilde{m}_1+N_h-f)} \binom{\tilde{m}_1+N_h-f-1}{N_h-f} \frac{\gamma_l(f,D_2x)}{\Gamma(f)(D_2)^f} - \sum_{b=0}^{\tilde{m}_1-1} \frac{(2)^{-b-N_h}\Gamma(b+N_h)}{\Gamma(b+1)\Gamma(N_h)} \\ &\Big[\sum_{f=1}^{\tilde{m}_1-b} (-1)^{\tilde{m}_1-b-f} (D_2/2-D_1/2)^{-(\tilde{m}_1+N_h-f)} \binom{\tilde{m}_1+N_h-f-1}{\tilde{m}_1-b-f} \frac{\gamma_l(f,D_1x)}{\Gamma(f)(D_1)^f} + \\ &\sum_{f=1}^{N_h+b} (-1)^{N_h+b-f} (D_1/2-D_2/2)^{-(\tilde{m}_1+N_h-f)} \binom{\tilde{m}_1+N_h-f-1}{N_h+b-f} \frac{\gamma_l(f,(D_1/2+D_2/2)x)}{\Gamma(f)((D_1/2+D_2/2))^f}\Big]\Big]. \end{aligned} \tag{20}$$

$$\begin{aligned}\mathrm{Per}\tilde{\boldsymbol{A}}_K = &\sum_{\substack{i_1,i_2,\ldots,i_{M-1}\\ 1\le i_1<i_2<\ldots<i_{M-1}\le M}} \sum_{q\in\mathbb{P}_p} \sum_{q_1=0}^{1} \cdots \sum_{q_{M-1}=0}^{1} \binom{1}{q_1} \cdots \binom{1}{q_{M-1}} (-1)^{q_1+\ldots+q_{M-1}} \\ &\sum_{\substack{q_{1,1},\ldots,q_{1,N_h}\\ q_{1,1}+\ldots+q_{1,N_h}=q_1}} \cdots \sum_{\substack{q_{M-K,1},\ldots,q_{M-K,N_h}\\ q_{M-1,1}+\ldots+q_{M-1,N_h}=q_{M-1}}} \prod_{j=1}^{M-1} \Big(\frac{q_j!}{q_{j,1}!\ldots q_{j,N_h}!}\Big) \\ &\prod_{j=1}^{M-1} \prod_{t_j=0}^{N_h-1} \Big(\frac{1}{t_j!}\Big)^{q_{j,t_j+1}} \prod_{j=1}^{M-1} \Big(\frac{1}{\tilde{\alpha}_{i,j}}\Big)^{\tilde{q}_j} \Big(\frac{1}{\tilde{\alpha}_{k_{1,q}}}\Big)^{N_h} \frac{e^{-x_1 D_1} x^{\tilde{m}-1}}{\Gamma(N_h)}. \end{aligned} \tag{21}$$

$$F_{S^{K=1}}(x) = \sum_{\substack{i_1,i_2,\ldots,i_{M-1}\\ 1\le i_1<i_2<\ldots<i_{M-1}\le M}} \sum_{q\in\mathbb{P}_p} \sum_{q_1=0}^{1} \cdots \sum_{q_{M-1}=0}^{1} \binom{1}{q_1}\cdots\binom{1}{q_{M-1}}(-1)^{q_1+\ldots+q_{M-1}}$$
$$\sum_{\substack{q_{1,1},\ldots,q_{1,N_h}\\ q_{1,1}+\ldots+q_{1,N_h}=q_1}} \cdots \sum_{\substack{q_{M-1,1},\ldots,q_{M-1,N_h}\\ q_{M-1,1}+\ldots+q_{M-1,N_h}=q_{M-1}}} \prod_{j=1}^{M-1}\Big(\frac{q_j!}{q_{j,1}!\ldots q_{j,N_h}!}\Big)$$
$$\prod_{j=1}^{M-1}\prod_{t_j=0}^{N_h-1}\Big(\frac{1}{t_j!}\Big)^{q_{j,t_j+1}} \prod_{j=1}^{M-1}\Big(\frac{1}{\tilde{\alpha}_{i,j}}\Big)^{\tilde{q}_j}\Big(\frac{1}{\tilde{\alpha}_{k_{1,q}}}\Big)^{N_h}\frac{1}{\Gamma(N_h)(D_1)^{\tilde{m}_1}}\underbrace{\gamma_l(\tilde{m}_1, D_1x)}_{K_1}. \tag{22}$$

$$P_e^{K=1} = \sum_{\substack{i_1,i_2,\ldots,i_{M-1}\\ 1\le i_1<i_2<\ldots<i_{M-1}\le M}} \sum_{q\in\mathbb{P}_p} \sum_{q_1=0}^{1} \cdots \sum_{q_{M-1}=0}^{1} \binom{1}{q_1}\cdots\binom{1}{q_{M-1}}(-1)^{q_1+\ldots+q_{M-1}}$$
$$\sum_{\substack{q_{1,1},\ldots,q_{1,N_h}\\ q_{1,1}+\ldots+q_{1,N_h}=q_1}} \cdots \sum_{\substack{q_{M-1,1},\ldots,q_{M-1,N_h}\\ q_{M-1,1}+\ldots+q_{M-1,N_h}=q_{M-1}}} \prod_{j=1}^{M-1}\Big(\frac{q_j!}{q_{j,1}!\ldots q_{j,N_h}!}\Big)\prod_{j=1}^{M-1}\prod_{t_j=0}^{N_h-1}\Big(\frac{1}{t_j!}\Big)^{q_{j,t_j+1}}$$
$$\prod_{j=1}^{M-1}\Big(\frac{1}{\tilde{\alpha}_{i,j}}\Big)^{\tilde{q}_j}\Big(\frac{1}{\tilde{\alpha}_{k_{1,q}}}\Big)^{N_h}\frac{m_a}{2\sqrt{\pi}\Gamma(N_h)(D_1)^{\tilde{m}_1}}G_{2,2}^{1,2}\Big(\frac{D_1}{m_b}\Big|\begin{matrix}1/2,1\\ \tilde{m}_1,0\end{matrix}\Big). \tag{25}$$

Finally, we note that $F_{S^{K=2}}(x)$ can be expressed in terms of the summation of a finite number of lower-incomplete gamma functions. This implies that the same approach as for the computation of $F_{S^{K=1}}(x)$ can be used. The resulting closed-form expression is not provided due to space limitations.

In the next section, simplified expressions of outage probability and ASER in i.i.d. frequency selective fading channels are provided.

IV. Performance Analysis in i.i.d. Frequency Selective Fading Channels

Let us assume a frequency elective fading channel, where each channel has the same number of multipath components. A closed-form expression of the CDF of S^K is provided in the following theorem.

Theorem 3: In i.i.d. frequency selective fading channels, the CDF of the aggregate received SNR from K CDD transmitters, is, for $K < M$ and $K = M$, respectively, given by (27) at the next page. In (27), we have defined $\beta \triangleq \frac{K}{1+p+K}$, $m_1 \triangleq N_hK - \tilde{l}$, $m_2 \triangleq \tilde{l} + \tilde{q} + N_h$, $\tilde{q} \triangleq \sum_{t=0}^{N_h-1} tq_{t+1}$ for a non-negative integer set $\{q_1, q_2, \ldots, q_{N_h}\}$ satisfying the condition $\sum_{k=1}^{N_h} q_k = p$ and $\tilde{l} \triangleq \sum_{t=0}^{N_h-1} tl_{t+1}$ for another non-negative integer set $\{l_1, l_2, \ldots, l_{N_h}\}$ satisfying the condition $\sum_{k=1}^{N_h} l_k = K$.

Proof: See Appendix C. ■

A. Outage Probability and Average Symbol Error Rate

With the aid of the CDF of S^K, the outage probability of the CDD-based CP-SC system can be formulated as follows:

$$\tilde{O}_{out}(\gamma_{\rm th}) = \tilde{F}_{S^K}(\gamma_{\rm th}). \tag{28}$$

Similar to the derivation of the ASER in i.n.i.d. frequency selective fading channels, the ASER in i.i.d. frequency selective fading channels is provided in the following theorem.

Theorem 4: In i.i.d. frequency selective fading channels, the ASER of the proposed CDD-based CP-SC system is given by (29) at the next page.

The details of the proof are omitted because it directly follows by applying the notable integral in (26).

B. Asymptotic Analysis of Outage Probability and Average Symbol Error Rate

To better understand the performance of the proposed scheme, we analyze the behavior of the CDF of S^K in the high-SNR regime. This is useful for identifying the diversity order of the system.

Proposition 1: In the high-SNR regime, the CDF of S^K can be simplified as follows:

$$\tilde{F}_{S^K}^{\rm as}(x) = K\binom{M}{K}\frac{\Gamma(MN_h - KN_h + N_h)}{\Gamma(N_h+1)^{M-K}\Gamma(N_h)} \frac{\gamma_l(MN_h, x/\tilde{\alpha})}{\Gamma(MN_h)}. \tag{30}$$

Proof: See Appendix D. ■

From *Proposition 1*, high-SNR expressions of outage probability and ASER can be obtained as follows:

$$\tilde{O}_{\rm out}^{\rm as}(\gamma_{\rm th}) = \tilde{F}_{S^K}^{\rm as}(\gamma_{\rm th}), \tag{31}$$

$$\tilde{P}_e^{K,\rm as} = K\binom{M}{K}\frac{\Gamma(MN_h - KN_h + N_h)}{\Gamma(N_h+1)^{M-K}\Gamma(N_h)}\frac{m_a}{2\sqrt{\pi}\Gamma(MN_h)} G_{2,2}^{1,2}\Big(\frac{1}{m_b\tilde{\alpha}}\Big|\begin{matrix}1/2,1\\ MN_h,0\end{matrix}\Big). \tag{32}$$

$$\tilde{F}_{S^{K<M}}(x) = \frac{M}{\Gamma(N_h)}\binom{M-1}{K}\sum_{p=0}^{M-K-1}\binom{M-K-1}{p}(-1)^p \sum_{\substack{q_1,\ldots,q_{N_h}\\ q_1+q_2+\ldots+q_{N_h}=p}} \frac{p!}{q_1!q_2!\ldots q_{N_h}!}$$
$$\sum_{\substack{l_1,\ldots,l_{N_h}\\ l_1+\ldots+l_{N_h}=K}} \frac{K!}{l_1!l_2!\ldots l_{N_h}!}\prod_{t_1=0}^{N_h-1}\Big(\frac{1}{t_1!}\Big)^{q_{t_1+1}}\prod_{t_2=0}^{N_h-1}\Big(\frac{1}{t_2!}\Big)^{l_{t_2+1}}\Gamma(\tilde{l}+\tilde{q}+N_h)(1+p+K)^{-\tilde{l}-\tilde{q}-N_h}$$
$$\Big[\sum_{f=1}^{m_1}(-1)^{m_1-f}\beta^{m_1-f}(1-\beta)^{-m_1-m_2+f}\binom{m_1+m_2-f-1}{m_1-f}$$
$$\frac{\gamma_l(f,\frac{x}{\tilde{\alpha}})}{\Gamma(f)} + \sum_{f=1}^{m_2}(-1)^{m_2-f}\beta^{m_1-f}(\beta-1)^{-m_1-m_2+f}\beta^f\binom{m_1+m_2-f-1}{m_2-f}\frac{\gamma_l(f,\frac{x}{\beta\tilde{\alpha}})}{\Gamma(f)}\Big],$$
$$\tilde{F}_{S^{K=M}}(x) = \frac{\gamma_l(MN_h, x/\tilde{\alpha})}{\Gamma(MN_h)}. \tag{27}$$

$$\tilde{P}_e^{K<M} = \frac{M}{\Gamma(N_h)}\binom{M-1}{K}\sum_{p=0}^{M-K-1}\binom{M-K-1}{p}(-1)^p \sum_{\substack{q_1,\ldots,q_{N_h}\\ q_1+q_2+\ldots+q_{N_h}=p}} \frac{p!}{q_1!q_2!\ldots q_{N_h}!}$$
$$\sum_{\substack{l_1,\ldots,l_{N_h}\\ l_1+\ldots+l_{N_h}=K}} \frac{K!}{l_1!l_2!\ldots l_{N_h}!}\prod_{t_1=0}^{N_h-1}\Big(\frac{1}{t_1!}\Big)^{q_{t_1+1}}\prod_{t_2=0}^{N_h-1}\Big(\frac{1}{t_2!}\Big)^{l_{t_2+1}}\Gamma(\tilde{l}+\tilde{q}+N_h)(1+p+K)^{-\tilde{l}-\tilde{q}-N_h}$$
$$\Big[\sum_{f=1}^{m_1}(-1)^{m_1-f}\beta^{m_1-f}(1-\beta)^{-m_1-m_2+f}\binom{m_1+m_2-f-1}{m_1-f}\frac{m_a}{2\sqrt{\pi}\Gamma(f)}G_{2,2}^{1,2}\Big(\frac{1}{m_b\tilde{\alpha}}\Big|\begin{matrix}1/2,1\\ f,0\end{matrix}\Big)+$$
$$\sum_{f=1}^{m_2}(-1)^{m_2-f}\beta^{m_1}(\beta-1)^{-m_1-m_2+f}\binom{m_1+m_2-f-1}{m_2-f}\frac{m_a}{2\sqrt{\pi}\Gamma(f)}G_{2,2}^{1,2}\Big(\frac{1}{m_b\beta\tilde{\alpha}}\Big|\begin{matrix}1/2,1\\ f,0\end{matrix}\Big)\Big],$$
$$\tilde{P}_e^{K=M} = \frac{m_a}{2\sqrt{\pi}\Gamma(MN_h)}G_{2,2}^{1,2}\Big(\frac{1}{m_b\tilde{\alpha}}\Big|\begin{matrix}1/2,1\\ MN_h,0\end{matrix}\Big). \tag{29}$$

Finally, from the asymptotic expressions of the outage probability and ASER, the achievable diversity order of the proposed CDD-based CP-SC transmission scheme is provided in the following theorem.

Theorem 5: The proposed distributed CDD-based CP-SC transmission schemes which specify the CDD delay according to two sufficient conditions provided by Eqs. (4) and (5) achieve a diversity order equal to $G_d = MN_h$, where M is the total number of transmitters available in the system and N_h is the number of multipath components of the channel.

Proof: We first approximate (31) as:

$$\tilde{O}_{\text{out}}^{\text{as}}(\gamma_{\text{th}}) \approx C_o K\binom{M}{K}\frac{\Gamma(MN_h-KN_h+N_h)}{\Gamma(N_h+1)^{M-K}\Gamma(N_h)}$$
$$\frac{(\gamma_{\text{th}}/\alpha)^{MN_h}}{\Gamma(MN_h+1)}\Big(\frac{P_T}{\sigma_z^2}\Big)^{-MN_h} \tag{33}$$

where C_o is an approximation constant.

We observe that $G_{p,q}^{m,n}\Big(z\Big|\begin{matrix}a_1,\cdots,a_n,a_{n+1},\cdots,a_p\\ b_1,\cdots,b_m,b_{m+1},\cdots,b_q\end{matrix}\Big) \propto z^\beta$ as $z\to 0$, where $\beta = \min(b_1,\ldots,b_m)$ [30, Section 5.4.1]. Based on this, we can approximate (32) as follows:

$$\tilde{P}_e^{K,\text{as}} \approx C_p K\binom{M}{K}\frac{\Gamma(MN_h-KN_h+N_h)}{\Gamma(N_h+1)^{M-K}\Gamma(N_h)}$$
$$\frac{m_a\alpha^{-MN_h}}{2\sqrt{\pi}\Gamma(MN_h)m_b^{MN_h}}\Big(\frac{P_T}{\sigma_z^2}\Big)^{-MN_h} \tag{34}$$

where C_p is an approximation constant. The proof follows by direct inspection of (33) and (34). ■

It is worth nothing that the constants C_o in (33) and C_p in (34) affect the accuracy of proposed asymptotic approximations, i.e., the coding gain, however they do not affect the diversity order.

Finally, we note that the number of cooperating CDD transmitters, K, does not affect the diversity order of the system. This is a novel finding with respect to past research works, such as [31]–[33]. In [33], the difference between the total number of transmitters, M, and the number of selected transmitters, K, determines the maximum diversity order [31], [32]. Our proposed system, on the other hand, is more similar to cooperative relaying, where the diversity order is a function of the total number of relays [15], [34].

V. Simulation Results

In this section, link-level simulations are conducted to validate analysis and findings. For simplicity, Binary Phase Shift Keying (BPSK) modulation is used. The curves obtained via link-level simulations are denoted by **Ex**. Analytical performance curves are denoted by **An**. High-SNR curves are denoted by **As**. The transmission block size for CP-SC transmission is $Q = 64$ with $N_p = 16$. The transmission power is assumed to be $P_T = 1$ for all transmitters. The SNR threshold causing an outage is $\gamma_{\rm th} = 3$ dB. Note that we consider the i.n.i.d. frequency selective fading channel and the i.i.d. frequency selective fading channel in order. Taking into account of transmitter cooperation, we compare the performance of this work with that of selection combining which was proposed by [20] and [35]. We can see that this selection combining is a special case of the proposed CDD scheme with $K = 1$.

A. Independent but non-identically distributed (i.n.i.d.) frequency selective fading channel

We choose a particular location of the receiver and six transmitters at the most, that is, $M = 6$. The pathloss components over the channels from the transmitters to receiver are given by $\alpha = \{0.12, 0.13, 0.14, 0.15, 0.16, 0.143\}$; that is, $\alpha_1 = 0.12, \ldots, \alpha_6 = 0.143$. The same number of multipath components for each channel is assumed.

1) Outage Probability Analysis: For this particular set of pathloss components, Figs. 2 and 3 show the accuracy of the derived outage probability obtained by using (23), when compared with the exact outage probability from simulations.

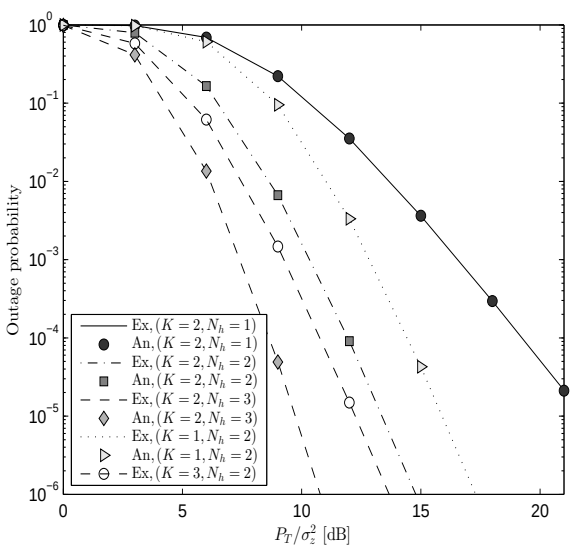

Fig. 2. Outage probability as a function of the number of multipath components and CDD transmitters. When $K = 1$, the outage probability corresponds to the CP-SC system with selection combining .

In Fig. 2, we investigate the effect of the number of multipath components and the number of CDD transmitters on the outage probability. This figure shows that the derived outage probability for various scenarios is very tight to that obtained via link-level simulations. For a fixed number of four transmitters and two CDD transmitters, a different number of multipath components results in a different outage probability. As the number of multipath components increases, for instance, $N_h = 3$ vs. $N_h = 1$, a steeper slope can be observed. Thus, we can infer from this figure that the number of multipath components is one of the key factors that determine the diversity gain. For a fixed number of four transmitters and two multipath components, this figure shows that a lower outage probability is obtained if more CDD transmitters are chosen. This is due to an increased aggregated signal power at the receiver. However, we can observe that the same slope is obtained, while the curves move to a lower outage probability region. This indicates that the number of CDD transmitters, K, influence the coding gain rather than the diversity gain. An example is given by the curves corresponding to the setups $(K = 3, N_h = 2)$ vs. $(K = 3, N_h = 1)$. Since the distributed CDD scheme can aggregate more signal power at the receiver as the number of CDD transmitters increases, the setup with a single CDD transmitter results in the worst outage probability. Note that the system proposed by [15] and [22] is somewhat similar to the set up of a single CDD transmitter, so that the distributed CDD scheme can provide a larger coding gain. In

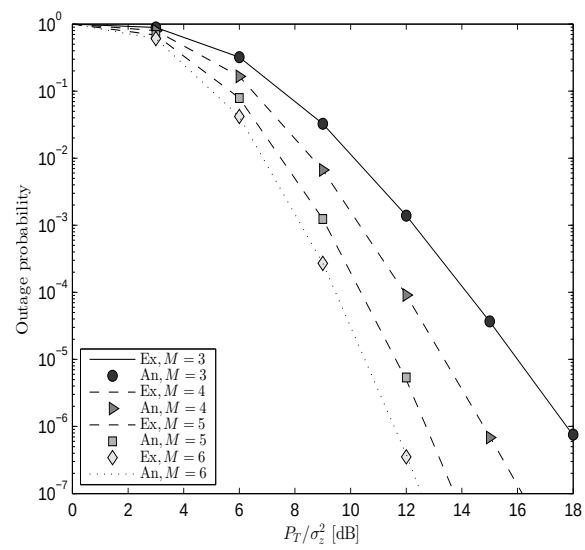

Fig. 3. Outage probability for several system setups.

Fig. 3, we investigate the effect of the number of transmitters on the outage probability. We assume two CDD transmitters and two multipath components. This figure shows that, as the number of transmitters increases, the distributed CDD scheme provides a smaller outage probability and a steeper curves's slope. An example is given by the setups $M = 6$ vs. $M = 2$. As the number of transmitters increases, it is more likely to get relative large channel gains, so that the distributed CDD scheme provides advantages on the aggregate signal power at the receiver. Thus, the number of transmitters in the system

is also a key factor in determining the slope of the outage probability, which corresponds to the diversity gain.

2) Average Symbol Error Rate Analysis: To validate our mathematical derivation of the ASER, we compare the derived ASER with that obtained by the QRD-M detector[4] [15], [36].

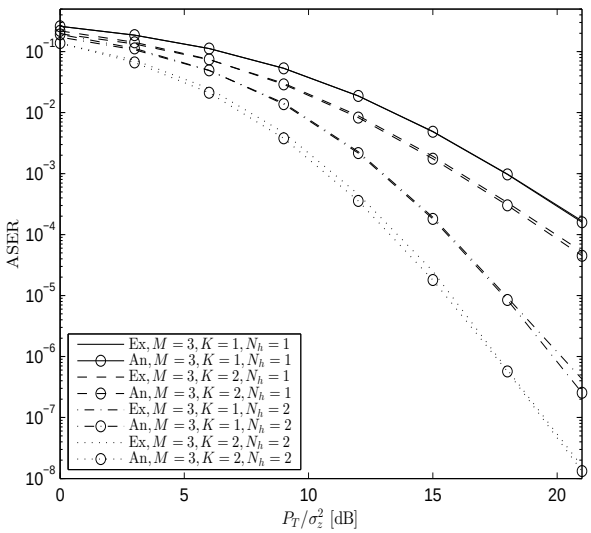

Fig. 4. ASER for several system setups. When $K = 1$, the ASER corresponds to the CP-SC system with selection combining.

Fig. 4 shows good agreement between the simulated ASER and the mathematical expression of the ASER for various values of K and N_h. This figure shows that as either the number of transmitters or the number of multipath components increases, a better ASER is obtained. Since using more CDD transmitters yields a higher aggregated signal power at the receiver, a better ASER is obtained as well.

In Fig. 5, we investigate the coding gain of the system by assuming a single CDD transmitter. Under the assumption of three multipath components, we observe that the ASEP gets better as the number of transmitters increases. An example if given by the setups $(M = 5, K = 1, N_h = 3)$ vs. $(M = 3, K = 1, N_h = 3)$. The case study $(M = 3, K = 1, N_h = 1)$, among those studied, provides the worst ASER. For a given slope (diversity order), we study the individual impact of K and N_h. From the figure, we note that the impact of multipath is more pronounced. Two setups showing these trends are $(M = 4, K = 1, N_h = 3)$ vs. $(M = 3, K = 1, N_h = 4)$, and $(M = 5, K = 1, N_h = 3)$ vs. $(M = 3, K = 1, N_h = 5)$.

B. Independent and identically distributed (i.i.d.) frequency selective fading channel

In this case, we assume $\alpha = 0.14$ for all path-losses.

1) Outage Probability Analysis: Fig. 6 compares the outage probability in (29) with simulations and show a good matching between them. Given the number of CDD transmitters and

[4]Interested readers can find relevant information about the QRD-M detector from [36].

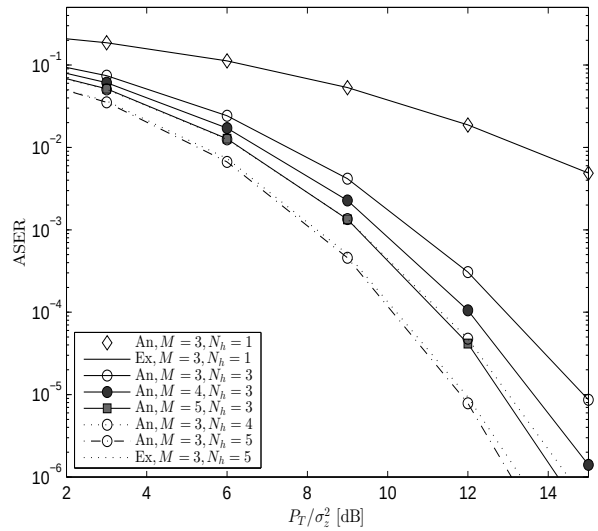

Fig. 5. ASER for several system setups.

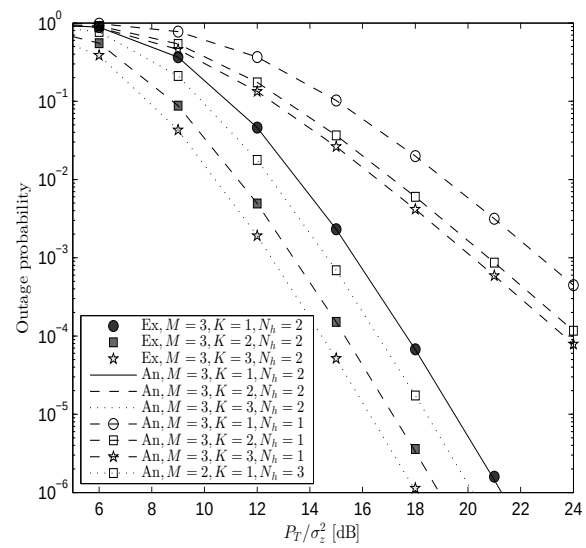

Fig. 6. Outage probability for various scenarios. When $K = 1$, the outage probability corresponds to the CP-SC system with selection combining.

the number of multipath components, we note that the slope of the curves (diversity order) does not change. In particular, two different slopes are shown in the figure: the setups $(M = 3, K = 1, N_h = 1)$, $(M = 3, K = 2, N_h = 1)$, and $(M = 3, K = 3, N_h = 1)$ have the same slope, whereas the setups $(M = 3, K = 1, N_h = 2)$, $(M = 3, K = 2, N_h = 2)$, $(M = 3, K = 3, N_h = 2)$, and $(M = 2, K = 1, N_h = 3)$ have a steeper slope than the other case studies. Once again, these numerical results confirm that the number of CDD transmitters do not affect the diversity order.

2) Average Symbol Error Rate Analysis: Similar to the i.n.i.d. frequency selective fading channel model, we compare the ASER of the proposed scheme against that obtained by us-

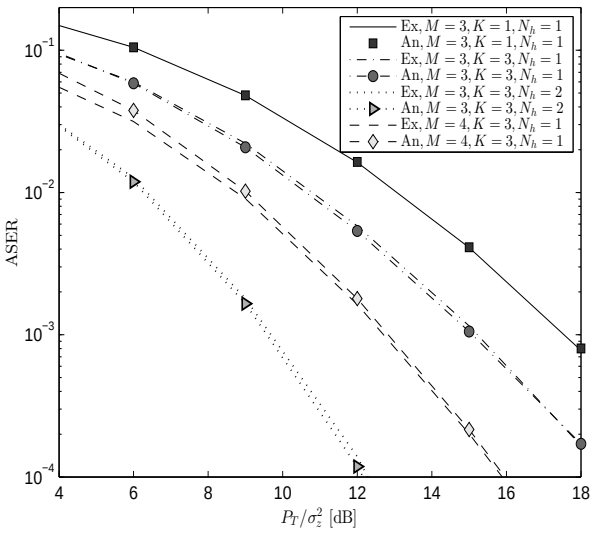

Fig. 7. ASER for several system setups. When $K = 1$, the ASER corresponds to the CP-SC system with selection combining.

ing the QRD-M detector. The results are reported in Fig. 7. For the considered case studies, e.g., $(M = 3, K = 1, N_h = 1)$, $(M = 3, K = 3, N_h = 1)$, $(M = 3, K = 3, N_h = 2)$, and $(M = 4, K = 3, N_h = 1)$, a good accuracy between modeling and simulations is obtained. In addition, this figure is obtained by using the same parameters used for the QRD-M demodulator in the i.n.i.d. frequency selective fading channel. This shows that the same diversity order is obtained.

C. Asymptotic Performance Analysis on Outage Probability and ASER

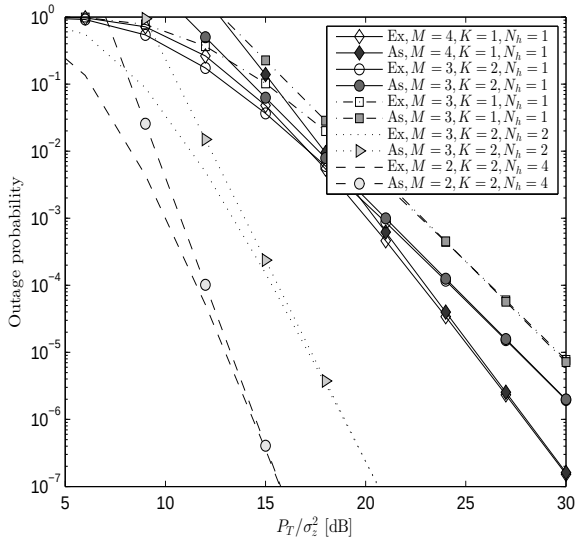

Fig. 8. Outage probability vs. asymptotic outage probability for several system setups. When $K = 1$, the outage probability corresponds to the CP-SC system with selection combining .

In Figs. 8 and 9, we compare the outage probability and ASER against their high-SNR asymptotic approximations. These two figures allow us to validate Theorem 5 and then to extract the maximum achievable diversity from the outage probability and ASER. As far as the approximations are concerned, we use the following constants: $C_o = 0.8$ for $(M = 4, K = 1, N_h = 1)$, $C_o = 0.25$ for $(M = 3, K = 2, N_h = 1)$, $C_o = 0.9$ for $(M = 3, K = 1, N_h = 1)$, $C_o = 0.15$ for $(M = 3, K = 2, N_h = 2)$, and $C_o = 0.65$ for $(M = 2, K = 2, N_h = 4)$. By using these values, we obtain a tight approximation and note, as expected, that the slope of the curves does not change. By direct inspection of the curves, we note that the slope of the curves of the high-SNR asymptotic approximation of the outage probability is equal to $G_d = MN_h$. In particular, the setups $(M = 4, K = 1, N_h = 1)$, $\{(M = 3, K = 2, N_h = 1), (M = 3, K = 1, N_h = 1)\}$, $(M = 3, K = 2, N_h = 2)$, and $(M = 2, K = 2, N_h = 4)$ have a diversity order equal to $G_d = 4$, $G_d = 3$, $G_d = 3$, $G_d = 6$, and $G_d = 8$, respectively.

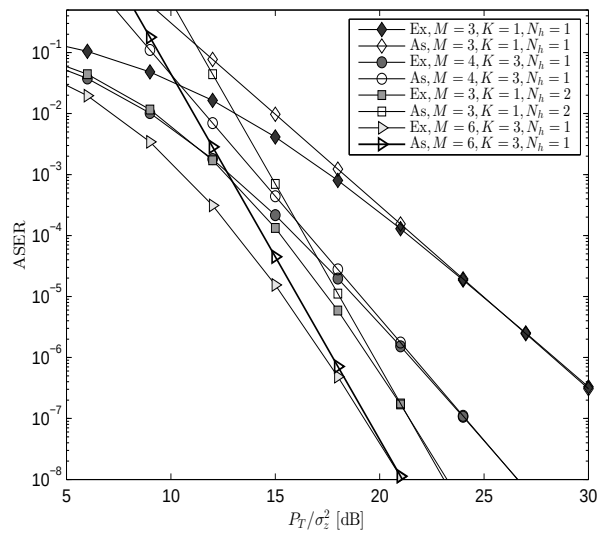

Fig. 9. ASER vs. asymptotic ASER for several system setups. When $K = 1$, the ASER corresponds to the CP-SC system with selection combining .

To produce the curves of the ASER in the high-SNR regime, we use the following constants: $C_p = 0.3$ for $(M = 4, K = 3, N_h = 1)$, $C_p = 25$ for $(M = 3, K = 2, N_h = 1)$, and $C_p = 0.4$ for $(M = 6, K = 3, N_h = 1)$. In this case as well, a good approximation is obtained in the high-SNR regime. Similar to the outage probability, the diversity gain is $G_d = MN_h$ and, in particular, the setups $(M = 3, K = 1, N_h = 1)$, $(M = 4, K = 3, N_h = 1)$, $(M = 3, K = 1, N_h = 2)$, $(M = 6, K = 3, N_h = 1)$, $(M = 3, K = 1, N_h = 2)$ and $(M = 6, K = 3, N_h = 1)$ provide the largest diversity order.

VI. Conclusions

In this paper, we have proposed a new distributed CDD-based CP-SC transmission scheme. Two conditions have been derived to achieve the maximum diversity at full rate, which allow us to suppress the interference caused by allowing

multiple transmitters to be active and by the time dispersion introduced by the channel. The outage probability and the ASER of the proposed scheme have been analyzed in i.n.i.d and i.i.d. frequency selective fading channels. It has been proved that the maximum diversity order of the system is equal to the product of the number of available transmitters and of the number of multipath components. With the aid of simulations, it has been shown that the number of CDD transmitters, on the other hand, affects the coding gain but it does not affect the diversity order.

Appendix A: Derivation of Proposition 1

It is known that the performance of a MLD depends on trace $\Big((\boldsymbol{H}_{cir}^{\Delta_k})^H \boldsymbol{H}_{cir}^{\Delta_k}\Big)$, which is given by

$$\begin{aligned}\text{trace}\Big((\boldsymbol{H}_{cir}^{\Delta_k})^H \boldsymbol{H}_{cir}^{\Delta_k}\Big) &= (\boldsymbol{R}^{\Delta_k}(1,1))^2 \\ &= (\boldsymbol{R}(1,1))^2 \\ &= \sum_{l=1}^{N} |\boldsymbol{h}_{cir}^{\Delta_k}(l)|^2 = \sum_{l=1}^{N} |\boldsymbol{h}_{cir}(l)|^2 \end{aligned} \quad \text{(A.1)}$$

where $\boldsymbol{h}_{cir}^{\Delta_k}$ and $\boldsymbol{h}_{cir}$ are the first column vectors of $\boldsymbol{H}_{cir}^{\Delta_k}$ and $\boldsymbol{H}_{cir}$, respectively, whose lth elements are denoted by $\boldsymbol{h}_{cir}^{\Delta_k}(l)$ and $\boldsymbol{h}_{cir}(l)$. Eq. (A.1) shows that the trace $\Big((\boldsymbol{H}_{cir}^{\Delta_k})^H \boldsymbol{H}_{cir}^{\Delta_k}\Big)$ is independent of the column permutations. This implies that the MLD provides the same performance for different assignments of the cyclic delays to the CDD transmitters, provided that each transmitter is assigned a different (unique) delay.

Appendix B: Derivation of Theorem 1

If $K = 2$, the MGF simplifies to:

$$\Phi_{S^{K=2}}(s) = \int_0^{x_2}\int_0^{\infty} e^{-s(x_1+x_2)} \text{Per}\tilde{\boldsymbol{A}}_K dx_1 dx_2 \quad \text{(B.1)}$$

which is evaluated as (B.2) at the next page. To compute (B.2), we have used the series expansion of the lower incomplete gamma function [25, eq. (8.352.1)]. The following equivalent expressions of J_2 and J_3 can be obtained:

$$\begin{aligned} J_2 = &\sum_{f=1}^{\tilde{m}_1} (-1)^{\tilde{m}_1-f}(D_2-D_1)^{-(\tilde{m}_1+N_h-f)} \\ &\binom{\tilde{m}_1+N_h-f-1}{\tilde{m}_1-f}(s+D_1)^{-f} + \sum_{f=1}^{N_h}(-1)^{N_h-f} \\ &(D_1-D_2)^{-(\tilde{m}_1+N_h-f)}\binom{\tilde{m}_1+N_h-f-1}{N_h-f}(s+D_2)^{-f} \end{aligned} \quad \text{(B.3)}$$

and

$$\begin{aligned} J_3 = &\sum_{f=1}^{\tilde{m}_1-b} (-1)^{\tilde{m}_1-b-f}\Big(\frac{D_2}{2}-\frac{D_1}{2}\Big)^{-(\tilde{m}_1+N_h-f)} \\ &\binom{\tilde{m}_1+N_h-f-1}{\tilde{m}_1-b-f}(s+D_1)^{-f} + \sum_{f=1}^{N_h+b}(-1)^{N_h+b-f} \\ &\Big(\frac{D_1}{2}-\frac{D_2}{2}\Big)^{-(\tilde{m}_1+N_h-f)}\binom{\tilde{m}_1+N_h-f-1}{N_h+b-f} \\ &\Big(s+\frac{D_1}{2}+\frac{D_2}{2}\Big)^{-f}. \end{aligned} \quad \text{(B.4)}$$

By applying the inverse MGF to J_2/s and J_3/s, the CDF can be expressed as the summations of the following two terms:

$$\begin{aligned} F_{J_2} = &\sum_{f=1}^{\tilde{m}_1}(-1)^{\tilde{m}_1-f}(D_2-D_1)^{-(\tilde{m}_1+N_h-f)} \\ &\binom{\tilde{m}_1+N_h-f-1}{\tilde{m}_1-f}\frac{\gamma_l(f,D_1x)}{\Gamma(f)(D_1)^f} + \sum_{f=1}^{N_h}(-1)^{N_h-f} \\ &(D_1-D_2)^{-(\tilde{m}_1+N_h-f)}\binom{\tilde{m}_1+N_h-f-1}{N_h-f} \\ &\frac{\gamma_l(f,D_2x)}{\Gamma(f)(D_2)^f} \end{aligned} \quad \text{(B.5)}$$

and

$$\begin{aligned} F_{J_3} = &\sum_{f=1}^{\tilde{m}_1-b}(-1)^{\tilde{m}_1-b-f}\Big(\frac{D_2}{2}-\frac{D_1}{2}\Big)^{-(\tilde{m}_1+N_h-f)} \\ &\binom{\tilde{m}_1+N_h-f-1}{\tilde{m}_1-b-f}\frac{\gamma_l(f,D_1x)}{\Gamma(f)(D_1)^f} + \sum_{f=1}^{N_h+b}(-1)^{N_h+b-f} \\ &\Big(\frac{D_1}{2}-\frac{D_2}{2}\Big)^{-(\tilde{m}_1+N_h-f)}\binom{\tilde{m}_1+N_h-f-1}{N_h+b-f} \\ &\frac{\gamma_l(f,(\frac{D_1}{2}+\frac{D_2}{2})x)}{\Gamma(f)(\frac{D_1}{2}+\frac{D_2}{2})^f}. \end{aligned} \quad \text{(B.6)}$$

Replacing J_2 and J_3 in (B.2) by F_{J_2} and F_{J_3}, we can readily obtain (20).

Appendix C: Derivation of Theorem 3

According to [37], conditioned on $\gamma_{(M-K)}$ and $\alpha = 1$, S^K can be written as a summation of K i.i.d. random variables as follows:

$$S^K|\gamma_{(M-K)} = \sum_{s=1}^{K}\gamma_s^* \quad \text{(C.1)}$$

where $\gamma_1^*, \cdots, \gamma_K^*$ are i.i.d. random variables whose PDF is

$$f_{\gamma^*}(y) = \frac{f_1(y)}{(1-F_1(x))} \text{ for } y > x \quad \text{(C.2)}$$

with $F_1(\cdot)$ and $f_1(\cdot)$ denoting, respectively, the CDF and PDF of γ_1. From (C.1), the PDF of S^K and its corresponding MGF can be formulated as follows:

$$\begin{aligned} f_{S^K}(y) &= \int_0^y f_{S^K|\gamma_{(M-K)}=x}(y|x) f_{\gamma_{(M-K)}}(x)dx \text{ and} \\ \Phi_{S^K}(s) &= \int_0^{\infty}\Phi_{\gamma^*}^K(s) f_{\gamma_{(M-K)}}(x)dx \end{aligned} \quad \text{(C.3)}$$

where $\Phi_{\gamma^*}(s)$ is the MGF of γ_1^*. From (C.2), $\Phi_{\gamma^*}(s)$ is given by

$$\begin{aligned} \Phi_{\gamma^*}(s) = &\frac{1}{(1+s)^{N_h}}\Big(1-F_1((1+s)x)\Big) \\ &(1-F_1(x))^{-1}. \end{aligned} \quad \text{(C.4)}$$

Applying the binomial and multinomial theorems [25, eq. (1.111)], $\Phi_{S^K}(s)$ is computed as in (C.5) at the next page.

$$\Phi_{S^{K=2}}(s) = \sum_{\substack{i_1,i_2,\ldots,i_{C-2}\\ 1\le i_1<i_2<\ldots<i_{C-2}\le C}} \sum_{q\in\mathbb{P}_p} \sum_{q_1=0}^{1} \cdots \sum_{q_{C-2}=0}^{1} \binom{1}{q_1}\cdots\binom{1}{q_{C-2}}(-1)^{q_1+\ldots+q_{C-2}}$$
$$\sum_{\substack{q_{1,1},\ldots,q_{1,N_h}\\ q_{1,1}+\ldots+q_{1,N_h}=q_1}} \cdots \sum_{\substack{q_{C-2,1},\ldots,q_{C-2,N_h}\\ q_{C-2,1}+\ldots+q_{C-2,N_h}=q_{C-2}}} \prod_{j=1}^{C-2}\Big(\frac{q_j!}{q_{j,1}!\ldots q_{j,N_h}!}\Big)\prod_{j=1}^{C-2}\prod_{t_j=0}^{N_h-1}\Big(\frac{1}{t_j!}\Big)^{q_{j,t_j+1}}$$
$$\prod_{j=1}^{C-2}\Big(\frac{1}{\tilde{\alpha}_{i,j}}\Big)^{\tilde{q}_j}\Big(\frac{1}{\tilde{\alpha}_{k_{1,q}}}\Big)^{N_h}\frac{\Gamma(\tilde{m}_1)}{\Gamma(N_h)}\Big(\frac{1}{\tilde{\alpha}_{k_{2,q}}}\Big)^{N_h}\Bigg[\underbrace{(s+D_1)^{-\tilde{m}_1}(s+D_2)^{-N_h}}_{J_2}$$
$$-\sum_{b=0}^{\tilde{m}_1-1}\frac{(2)^{-b-N_h}\Gamma(b+N_h)}{\Gamma(N_h)\Gamma(b+1)}\underbrace{(s+D_1)^{-(\tilde{m}_1-b)}\Big(s+\frac{D_1}{2}+\frac{D_2}{2}\Big)^{-(b+N_h)}}_{J_3}\Bigg]. \tag{B.2}$$

$$\Phi_{S^K}(s) = \frac{M}{\Gamma(N_h)}\binom{M-1}{K}\sum_{p=0}^{M-K-1}\binom{M-K-1}{p}(-1)^p\sum_{q_1,\ldots,q_{N_h}}\frac{p!}{q_1!\ldots q_{N_h}!}\sum_{l_1,\ldots,l_{N_h}}\frac{K!}{l_1!\ldots l_{N_h}!}$$
$$\prod_{t_1=0}^{N_h-1}\Big(\frac{1}{t_2!}\Big)^{q_{t_1+1}}\prod_{t_2=0}^{N_h-1}\Big(\frac{1}{t_2!}\Big)^{l_{t_2+1}}\Gamma(\tilde{l}+\tilde{q}+N_h)(1+p+K)^{-\tilde{l}-\tilde{q}-N_h}\underbrace{(1+s)^{-m_1}(1+\beta s)^{-m_2}}_{J_4}. \tag{C.5}$$

$$\Phi_{S^K}(s) = \frac{M}{\Gamma(N_h)}\binom{M-1}{K}\sum_{p=0}^{M-K-1}\binom{M-K-1}{p}(-1)^p\sum_{q_1,\ldots,q_{N_h}}\frac{p!}{q_1!\ldots q_{N_h}!}\sum_{l_1,\ldots,l_{N_h}}\frac{K!}{l_1!\ldots l_{N_h}!}\prod_{t_1=0}^{N_h-1}\Big(\frac{1}{t_1!}\Big)^{q_{t_1+1}}$$
$$\prod_{t_2=0}^{N_h-1}\Big(\frac{1}{t_2!}\Big)^{l_{t_2+1}}\Gamma(\tilde{l}+\tilde{q}+N_h)(1+p+K)^{-\tilde{l}-\tilde{q}-N_h}\Big(\sum_{i=1}^{m_1}(-1)^{m_1-i}\beta^{m_1-i}(1-\beta)^{-m_1-m_2+i}$$
$$\binom{m_1+m_2-i-1}{m_1-i}(1+s)^{-i}+\sum_{i=1}^{m_2}(-1)^{m_2-i}\beta^{m_1-i}(\beta-1)^{-m_1-m_2+i}\binom{m_1+m_2-i-1}{m_2-i}\Big(\frac{1}{\beta}+s\Big)^{-i}\Big). \tag{C.6}$$

Applying the partial fraction (PF) to J_4 w.r.t. s, (C.5) can be expressed as (C.6). By applying the inverse MGF of $\Phi_{S^K}(s)/s$ w.r.t. s, the CDF of S^K can be derived.

Appendix D: Derivation of Proposition 1

Consider the following different but equivalent expression for the MGF of S^K:

$$M_{S^K}(s) = \frac{K\binom{M}{K}}{(1+s)^{N_hK}}\int_0^\infty\Big(F_1\Big(\frac{x}{1+s}\Big)\Big)^{M-K}(1-F_1(x))^{K-1}f_1(x)dx \tag{D.1}$$

where we assume $\alpha = 1$. In the high SNR region, we can approximate $1-F_1(x)$ and $F_1(x)$ by their asymptotic expressions [33] as:

$$1-F_1(x)\overset{x\to 0}{\approx}1 \text{ and } F_1(x)\overset{x\to 0}{\approx}\frac{x^{N_h}}{\Gamma(N_h+1)} \tag{D.2}$$

so that we have the following asymptotic approximation for (D.1):

$$M^{\text{as}}_{S^K}(s) = \frac{K\binom{M}{K}}{(1+s)^{MN_h}}\frac{1}{\Gamma(N_h+1)^{M-K}\Gamma(N_h)}\int_0^\infty x^{MN_h-KN_h+N_h-1}e^{-x}dx$$
$$= K\binom{M}{K}\frac{\Gamma(MN_h-KN_h+N_h)}{\Gamma(N_h+1)^{M-K}\Gamma(N_h)}(1+s)^{-MN_h}. \tag{D.3}$$

Thus, the high-SNR expression of the CDF of S^K is as follows:

$$\tilde{F}^{\text{as}}_{S^K}(x) = K\binom{M}{K}\frac{\Gamma(MN_h-KN_h+N_h)}{\Gamma(N_h+1)^{M-K}\Gamma(N_h)}\frac{\gamma_l(MN_h,x)}{\Gamma(MN_h)}. \tag{D.4}$$

References

[1] J. K. Cavers, "Single-user and multiuser adaptive maximal ratio transmission for Rayleigh channels," *IEEE Trans. Veh. Technol.*, vol. 49, no. 6, pp. 2043–2050, Nov. 2000.

[2] T. K. Y. Lo, "Maximum ratio transmission," *IEEE Trans. Commun.*, vol. 47, no. 10, pp. 1458–1461, Oct. 1999.

[3] K. J. Kim, T. Khan, and P. Orlik, "Performance analysis of cooperative systems with unreliable backhauls and selection combining," *IEEE Trans. Veh. Technol.*, vol. 66, no. 3, pp. 2448–2461, Mar. 2017.

[4] J. N. Laneman and G. W. Wornell, "Energy-efficient antenna sharing and relaying for wireless networks," in *Proc. IEEE Wireless Communications and Networking Conf.*, Chicago, IL, Oct. 2000, pp. 7–12.

[5] M. O. Astal and A. M. Abu-Hudrouss, "SIC detector for 4 relay distributed space-time block coding under quasi-synchronization," *IEEE Commun. Lett.*, vol. 15, no. 10, pp. 1056–1058, Oct. 2011.

[6] Y.-C. Liang, W. S. Leon, Y. Zeng, and C. Xu, "Design of cyclic delay deievsity for single carrier cyclic prefix (sccp) transmissions with block-iterative GDFE (BI-GDFE) receiver," *IEEE Trans. Wireless Commun.*, vol. 7, no. 2, pp. 677–684, Feb. 2008.

[7] A. H. Mehana and A. Nosratinia, "Single-carrier frequency-domain equalizer with multi-antenna transmit diversity," *IEEE Trans. Wireless Commun.*, vol. 12, pp. 388–397, Jan. 2013.

[8] F. Zhang, Y. Zhang, W. Q. Malik, B. Allen, and D. J. Edwards, "Optimum receiver antenna selection for transmit cyclic delay diversity," in *Proc. IEEE Int. Conf. Commun.*, Beijing, China, May 2008, pp. 3829–3833.

[9] U.-K. Kwon and G.-H. Im, "Cyclic delay diversity with frequency domain Turbo equalization for uplink fast fading channels," *IEEE Commun. Lett.*, vol. 13, no. 3, pp. 184–186, Mar. 2009.

[10] Q. Li, Q. Yan, K. C. Keh, K. H. Li, and Y. Hu, "A multi-relay-selection scheme with cyclic delay diversity," *IEEE Commun. Lett.*, vol. 17, no. 2, pp. 349–352, Feb. 2013.

[11] IEEE, "Wireless LAN medium access control (MAC) and physical layer (PHY) specifications–Amendment 4: Enhancements for very high throughput for operation in bands below 6 GHz," *IEEE Standard 802.11ac-2013, Part 11*, 2009.

[12] ——, "Wireless LAN medium access control (MAC) and physical layer (PHY) specifications - Amendment 5: Enhancements for higher throughput," *IEEE Standard 802.11n-2009, Part 11*, 2009.

[13] 3GPP, Technical Specification Group Radio Access Network, "Evolved universal terrestrial radio access (E-UTRA): Physical channels and modulation (release 8)," *3GPP TS 36.211 V8.9.0 (2009-12) Technical Specification*, Mar. 2009.

[14] S. Kato, H. Harada, R. Funada, T. Baykas, C. S. Sum, J. Wang, and M. A. Rahman, "Single carrier transmission for multi-gigabit 60-GHz WPAN systems," *IEEE J. Sel. Areas Commun.*, vol. 27, no. 8, pp. 1466–1478, Oct. 2009.

[15] K. J. Kim and T. A. Tsiftsis, "On the performance of cyclic prefix-based single-carrier cooperative diversity systems with best relay selection," *IEEE Trans. Wireless Commun.*, vol. 10, no. 4, pp. 1269–1279, Apr. 2011.

[16] H. Eghbali, S. Muhaidat, and N. Al-Dhahir, "A novel receiver design for single-carrier frequency domain equalization in broadband wireless networks with amplify-and-forward relaying," *IEEE Trans. Wireless Commun.*, vol. 10, no. 3, pp. 721–727, Mar. 2011.

[17] H. Chergui, T. Ait-Idir, M. Benjillali, and S. Saoudi, "Joint-over-transmissions project and forward relaying for single carrier broadband MIMO ARQ systems," in *Proc. IEEE Veh. Techol. Conf.*, Yokohama, Japan, May 2011, pp. 1–5.

[18] H. Mheidat, M. Uysal, and N. Al-Dhahir, "Equalization techniques for distributed space-time block codes with amplify-and-forward relaying," *IEEE Trans. Signal Process.*, vol. 55, no. 5, pp. 1839–1852, May 2007.

[19] K. J. Kim, T. Q. Duong, and H. V. Poor, "Outage probability of single-carrier cooperative spectrum sharing systems with decode-and-forward relaying and selection combining," *IEEE Trans. Wireless Commun.*, vol. 12, no. 2, pp. 806–817, Feb. 2013.

[20] K. J. Kim, P. L. Yeoh, P. Orlik, and H. V. Poor, "Secrecy performance of finite-sized cooperative single carrier systems with unreliable backhaul connections," *IEEE Trans. Signal Process.*, vol. 64, no. 17, pp. 4403–4416, Sep. 2016.

[21] D. Falconer, S. L. Ariyavisitakul, A. B. Seeyar, and B. Eidson, "Frequency domain equalization for Single-Carrier broadband wireless systems," *IEEE Commun. Magazine*, pp. 58–66, Apr. 2002.

[22] K. J. Kim, T. A. Tsiftsis, and H. V. Poor, "Power allocation in cyclic prefixed single-carrier relaying systems," *IEEE Trans. Wireless Commun.*, vol. 10, no. 7, pp. 2297–2305, Jul. 2011.

[23] H. A. David and H. N. Nagaraja, *Order Statistics*, 3rd ed. Hoboken, New Jersey: John Wiley and Sons, 2005.

[24] N. Balakrishnan, "Permanents, order statistics, outliers, and robustness," *Rev. Mat. Complu.*, vol. 20, pp. 7–107, 2007.

[25] I. S. Gradshteyn and I. M. Ryzhik, *Table of Integrals, Series, and Products*. New York: Academic Press, 2007.

[26] H. Yu, I.-H. Lee, and G. L. Stuber, "Outage probability of decode-and-forward cooperative relaying systems with co-channel interference," *IEEE Trans. Wireless Commun.*, vol. 11, no. 1, pp. 266–274, Jan. 2011.

[27] H. A. Suraweera, P. J. Smith, and M. Shafi, "Capacity limits and performance analysis of cognitive radio with imperfect channel knowledge," *IEEE Trans. Veh. Technol.*, vol. 59, pp. 1811–1822, May 2010.

[28] Wolfman research inc. [Online]. Available: http://functions.wolfman.com

[29] A. P. Prudnikov, Y. A. Brychkov, and O. I. Marichev, *Integral and Series. Vol. 3: More Special Functions*, 3rd ed. London: Gordon and Breach, 1992.

[30] A. Erdelyi, *Higher Transcendental Functions*. New York, N.Y.: McGraw-Hill Book Company, 1953.

[31] S. S. Ikki and M. H. Ahmed, "On the performance of cooperative-diversity networks with the Nth best-relay selection scheme," *IEEE Trans. Commun.*, vol. 58, no. 11, pp. 3062–3069, Nov. 2010.

[32] S.-I. Chu, "Performance of amplify-and-forward cooperative communications with the Nth best-relay selection scheme over Nakagami-m fading channels," *IEEE Commun. Lett.*, vol. 15, no. 2, pp. 172–174, Feb. 2011.

[33] X. Zhang, Y. Zhang, Z. Yan, J. Xing, and W. Wang, "Performance analysis of cognitive relay networks over Nakagami-m fading channels," *IEEE J. Sel. Areas Commun.*, vol. 33, pp. 865–877, May 2016.

[34] F. A. Onat, Y. Fan, H. Yanikomeroglu, and H. V. Poor, "Threshold-based relay selection for decode-and-forward relaying in cooperative wireless networks," *EURASIP Journal on Wireless Communications and Networking*, vol. 2010:721492, pp. 1–9, 2010.

[35] N. Yang, P. L. Yeoh, M. Elkashlan, R. Schober, and I. B. Collings, "Transmit antenna selection for security enhancement in MIMO wiretap channels," *IEEE Trans. Commun.*, vol. 61, no. 1, pp. 144–154, Jan. 2013.

[36] K. J. Kim, Y. Yue, R. A. Iltis, and J. D. Gibson, "A QRD-M/Kalman Filter-based detection and channel estimation algorithm for MIMO-OFDM systems," *IEEE Trans. Wireless Commun.*, vol. 4, pp. 710–721, Mar. 2005.

[37] K. Alam and K. T. Wallenius, "Distribution of a sum of order statistics," *Scandinavian Journal of Statistics*, vol. 6, no. 3, pp. 845–855, 1979.

View publication stats